Laser under ultrastrong light-matter interaction: Qualitative aspects and quantitative influences by level and mode truncations

Motoaki Bamba* and Tetsuo Ogawa
Department of Physics, Osaka University, 1-1 Machikaneyama, Toyonaka, Osaka 560-0043, Japan
(Received 16 October 2014; revised manuscript received 26 January 2016; published 7 March 2016)

We investigate theoretically the light amplification by stimulated emission of radiation (laser) in the ultrastrong light-matter interaction regime under the two-level and single-mode approximations. The conventional picture of the laser is broken under the ultrastrong interaction. Instead, we must explicitly discuss the dynamics of the electric field and of the magnetic one distinctively, which make the "laser" qualitatively different from the conventional laser. We found that the laser generally accompanies odd-order harmonics of the electromagnetic fields both inside and outside the cavity and a synchronization with an oscillation of atomic population. A bistability is also demonstrated. However, since our model is quite simplified, we got quantitatively different results from the Hamiltonians in the velocity and length forms of the light-matter interaction, while the appearance of the multiple harmonics and the bistability is qualitatively reliable.

DOI: 10.1103/PhysRevA.93.033811

I. INTRODUCTION

The light and microwave amplifications by stimulated emission of radiation (laser and maser) were realized in 1960 [1] and 1958 [2], respectively. Although the fundamental theory for them is established up to the quantum fluctuations of light and microwave [3–6], the discussion is performed basically under the rotating-wave approximation (RWA) to the interaction between the electromagnetic fields and matter. Under the RWA, the total number of photons and atomic excitations is conserved during the interaction, and it has enabled the simple picture based on the photons and excitations. However, the RWA fails in the ultrastrong interaction regime, which shows vacuum Rabi splitting comparable to transition frequency of the atomic excitation [7] and can now be realized in a variety of systems experimentally [8–18]. In this regime, we will see that dynamics of the electric field and of the magnetic one should be discussed distinctively due to the lack of the RWA, and we can no longer describe the laser by the stimulated emission of radiation without the distinction. Resulting from this additional degree of freedom originating from the distinction, the "laser" and "maser" in the ultrastrong regime are expected to show essential differences from the conventional laser.

The additional degree of freedom appears in the equations of the laser (including the meaning of maser in the followings), and we will see that the laser solutions must have multiple harmonics for satisfying them. Due to the complicated equations with the multiharmonic expansion, we can find a rich variety of laser solutions that were hidden under the RWA in the conventional laser theory. In other words, the recovery of the original distinction of the electromagnetic fields in the ultrastrong regime brings out the multiple harmonics and the rich solutions. This is the conclusion of this paper, and we will show, as a demonstration, that bistable laser solutions are obtained even by a basic calculation.

In order to highlight the qualitative and essential aspects of the laser in the ultrastrong regime, we suppose an ensemble of all identical two-level atoms interacting with a single mode in a cavity of the electromagnetic fields, which has been considered to catch the basic properties of the conventional laser [3–6]. This simple system keeps the generality of the conventional laser theory, although it is known [11,19,20] that the finite-level and finite-mode approximations (truncation of higher levels and modes) in the ultrastrong regime are not suitable for pursuing the quantitative reliability, which is obtained only by specifying a particular system of interest. Instead, the calculations in this paper are performed in two typical forms of the light-matter interaction: the velocity and length forms (sometimes called the Coulomb and electric dipole gauges while both are in the Coulomb gauge in the sense of completely transverse vector potential $\nabla \cdot \boldsymbol{A} = 0$) [21–24]. The qualitative and general properties should be obtained independently of the form choice, which, however, gives us quantitatively different results.

In Sec. II, we show the equations for investigating the laser in the ultrastrong light-matter interaction regime. Its qualitative aspects (multiple harmonics and bistability) are discussed in Sec. III. The quantitative influence by the two-level and single-mode approximation is discussed in Sec. IV. The summary is given in Sec. V. In Appendix A, we briefly explain the framework of stochastic differential equations, by which the laser equations are derived, and we also show the Hamiltonian of system-environment couplings. The detailed calculations of the oscillating steady states from the laser equations are shown in Appendixes B and C for the velocity and length forms, respectively.

II. LASER EQUATIONS

Under the two-level, single-mode, and long-wavelength approximations, the system Hamiltonians are obtained in the velocity and length forms, respectively, as [24,25]

$$\hat{H}_0^v = \hbar\omega_c \hat{a}^\dagger \hat{a} + \sum_{\lambda=1}^{N} \frac{\hbar\omega_a}{2} \hat{\sigma}_\lambda^z + \frac{g\hbar\omega_a}{\sqrt{N}} (\hat{a} + \hat{a}^\dagger) \sum_{\lambda=1}^{N} \hat{\sigma}_\lambda^y + g^2 \hbar\omega_a (\hat{a} + \hat{a}^\dagger)^2, \quad (1)$$

*Present address: Department of Materials Engineering Science, Osaka University, 1-3 Machikaneyama, Toyonaka, Osaka 560-8531, Japan; bamba@qi.mp.es.osaka-u.ac.jp

$$\hat{H}_0^l = \hbar\omega_c \hat{a}^\dagger \hat{a} + \sum_{\lambda=1}^{N} \frac{\hbar\omega_a}{2} \hat{\sigma}_\lambda^z - \frac{ig\hbar\omega_c}{\sqrt{N}} (\hat{a} - \hat{a}^\dagger) \sum_{\lambda=1}^{N} \hat{\sigma}_\lambda^x + \frac{g^2\hbar\omega_c}{N} \sum_{\lambda=1}^{N} \sum_{\lambda'=1}^{N} \hat{\sigma}_\lambda^x \hat{\sigma}_{\lambda'}^x. \quad (2)$$

Here, ω_c is the frequency of the cavity mode, and ω_a is the atomic transition frequency. $\hat{a}$ is the annihilation operator of a photon in the cavity mode and satisfies $[\hat{a},\hat{a}^\dagger] = 1$, while the photon does not provide a good picture in the ultrastrong regime. N is the number of atoms, and $\hat{\sigma}_\lambda^{x,y,z}$ is the Pauli matrix representing the λth atom. g is a nondimensional interaction strength:

$$g = \sqrt{\frac{\rho|d|^2}{2\varepsilon_0\hbar\omega_c}}, \quad g' = g\sqrt{\frac{\omega_c}{\omega_a}} = \sqrt{\frac{\rho|d|^2}{2\varepsilon_0\hbar\omega_a}}, \quad (3)$$

where d is the transition dipole moment of the atomic transition, ε_0 is the vacuum permittivity, and ρ is the density of atoms. In this paper, we define the ultrastrong regime as $g' \gtrsim 1$, which is determined only by the atomic parameters.

Under the RWA, the counterrotating terms $\hat{a}\hat{\sigma}_\lambda$ and $\hat{a}^\dagger\hat{\sigma}_\lambda^\dagger$ are neglected in the interaction Hamiltonians [$\hat{\sigma}_\lambda = (\hat{\sigma}_\lambda^x - i\hat{\sigma}_\lambda^y)/2$ is lowering operator of λth atom], and the total number of photons and atomic excitations is conserved in the remaining terms $\hat{a}^\dagger\hat{\sigma}_\lambda$ and $\hat{\sigma}_\lambda^\dagger\hat{a}$. Thanks to this simplification, in the conventional laser theory, we need to consider only the following three variables: the light amplitude $\langle\hat{a}\rangle/\sqrt{N}$, the atomic one $\sum_\lambda\langle\hat{\sigma}_\lambda\rangle/N$, and the atomic population $Z = \sum_\lambda\langle\hat{\sigma}_\lambda^z\rangle/2N$ [3–6]. However, in the ultrastrong regime, this simple picture is no longer appropriate ($\hat{a}$ and $\hat{\sigma}_\lambda$ no longer correspond to positive-frequency components or lowering operators of the system) due to the lack of the RWA. Instead, we need to consider the following five variables distinctively: the nondimensional vector potential $\mathcal{A} = \langle\hat{a} + \hat{a}^\dagger\rangle/\sqrt{N}$, electric field (or displacement) $\Pi = i\langle\hat{a} - \hat{a}^\dagger\rangle/\sqrt{N}$, atomic polarization $X = \sum_\lambda\langle\hat{\sigma}_\lambda^x\rangle/2N$, current $Y = \sum_\lambda\langle\hat{\sigma}_\lambda^y\rangle/2N$, and population Z. Thanks to this distinction, or the additional degrees of freedom, we can find unconventional solutions of complicated laser equations in the ultrastrong regime.

The inverted population is inevitable for the laser in our system even in the ultrastrong regime, and it corresponds to $Z > 0$, while $|Z| \leqslant 1/2$. Here, we introduce heat baths for pumping the atoms incoherently and also a bath for dissipation of the electromagnetic fields, whose couplings are mediated by $\hat{\sigma}_\lambda^x$ and $(\hat{a} + \hat{a}^\dagger)$, respectively, for suppressing the dependence on the form choice [26,27]. Without the electromagnetic interaction with matter, each atom is incoherently pumped to Z_p with a rate $\gamma_\parallel$ [6], and the electromagnetic fields decay with a rate κ. We also consider baths for pure dephasing of atomic amplitudes X and Y (including the influence of broadening of atomic transition frequencies), and they are mediated by $\hat{\sigma}_\lambda^z$ with a rate $\gamma_{\rm pure}$. These dissipation rates are supposed to be frequency independent for simplicity.

In the presence of these system-environment couplings, we derived quantum stochastic differential equations [6,26] based on the positive and negative frequency components [26,28] (see also Appendix A). For large enough $N \gg 1$ [6], macroscopic laser equations factorized by the above five variables are obtained in the velocity and length forms, respectively, as

$$(\partial/\partial t)\bar{\mathcal{A}} = -\omega_c\bar{\Pi}, \quad (4a)$$

$$(\partial/\partial t)\bar{\Pi} = (\omega_c + 4g^2\omega_a)\bar{\mathcal{A}} - i\kappa[\bar{\mathcal{A}}^{(+)} - \bar{\mathcal{A}}^{(-)}] + 4g\omega_a\bar{Y}, \quad (4b)$$

$$(\partial/\partial t)\bar{X} = -\gamma_x\bar{X} - \omega_a\bar{Y} + 2g\omega_a\bar{\mathcal{A}}\bar{Z}, \quad (4c)$$

$$(\partial/\partial t)\bar{Y} = \omega_a\bar{X} - \gamma_y\bar{Y}, \quad (4d)$$

$$(\partial/\partial t)\bar{Z} = -\gamma_z(\bar{Z} - Z_p) - 2g\omega_a\bar{\mathcal{A}}\bar{X}, \quad (4e)$$

$$(\partial/\partial t)\tilde{\mathcal{A}} = -\omega_c\tilde{\Pi} + 4g\omega_c\tilde{X}, \quad (5a)$$

$$(\partial/\partial t)\tilde{\Pi} = \omega_c\tilde{\mathcal{A}} - i\kappa[\tilde{\mathcal{A}}^{(+)} - \tilde{\mathcal{A}}^{(-)}], \quad (5b)$$

$$(\partial/\partial t)\tilde{X} = -\gamma_x\tilde{X} - \omega_a\tilde{Y}, \quad (5c)$$

$$(\partial/\partial t)\tilde{Y} = (\omega_a - 8g^2\omega_c\tilde{Z})\tilde{X} - \gamma_y\tilde{Y} + 2g\omega_c\tilde{\Pi}\tilde{Z}, \quad (5d)$$

$$(\partial/\partial t)\tilde{Z} = -\gamma_z(\tilde{Z} - Z_p) - 2g\omega_c\tilde{\Pi}\tilde{Y} + 8g^2\omega_c\tilde{X}\tilde{Y}. \quad (5e)$$

Here, the variables in the velocity form are distinguished by an overbar, for example, $\bar{\mathcal{A}}$, and those in the length form are distinguished by a tilde, for example, $\tilde{\mathcal{A}}$. The superscript $(\pm)$ means the positive and negative frequency components of the variables, based on which we get asymmetric dissipation rates: κ only for Π, $\gamma_x = \gamma_{\rm pure}$, $\gamma_y = \gamma_\parallel + \gamma_{\rm pure}$, and $\gamma_z = \gamma_\parallel$ [29].

III. QUALITATIVE ASPECTS OF THE LASER

In the conventional laser, the electromagnetic and atomic amplitudes ($\mathcal{A}$,Π,X, and Y) oscillate with a frequency Ω (determined for satisfying the laser equations), and the atomic population Z is constant in time. In contrast, in the ultrastrong regime, since the RWA cannot be applied to $2g\omega_a\bar{\mathcal{A}}(t)\bar{X}(t)$ in Eq. (4e) and also to $2g\omega_c\tilde{\Pi}(t)\tilde{Y}(t)$ in Eq. (5e), the atomic populations $\bar{Z}(t)$ and $\tilde{Z}(t)$ are driven not only by the time-constant components but also by the 2Ω ones, when the amplitudes oscillate with a fundamental frequency Ω. Further, $\bar{X}$ and $\tilde{Y}$ are driven by 3Ω components through $2g\omega_a\bar{\mathcal{A}}(t)\bar{Z}(t)$ in Eq. (4c) and $2g\omega_c\tilde{\Pi}(t)\tilde{Z}(t)$ in Eq. (5d), respectively. Therefore, the electromagnetic and atomic amplitudes in general oscillate with odd-order harmonics Ω, 3Ω, 5Ω, ..., and the atomic population oscillates with even-order harmonics 0Ω, 2Ω, 4Ω, ... Since the cavity loss is mediated by $\mathcal{A}$, the dynamics of the frequency components $\mathcal{A}^{(\pm)}(t)$ reflect those of the output from the cavity through the input-output relation [6,26,28,30]. Then, the output also oscillates with the odd-order harmonics. These multiple harmonics and synchronization with the atomic population are obtained in general. They are a part of the qualitative differences from the conventional laser and are obtained independently of the choice of the light-matter interaction form.

For simplicity, we consider only up to the third-order harmonic, which is sufficient for finding bistable laser solutions. The electromagnetic and atomic amplitudes are expanded as $\mathcal{A}(t) = \alpha_1 e^{-i\Omega t} + \alpha_3 e^{-i3\Omega t} + \text{c.c.}$, $\Pi(t) = p_1 e^{-i\Omega t} + p_3 e^{-i3\Omega t} + \text{c.c.}$ (and similarly for X and Y), and the atomic population is expanded as $Z(t) = Z_0 + (z_2 e^{-i2\Omega t} + \text{c.c.})$. Neglecting highly oscillating terms (RWA in the oscillation basis), nontrivial oscillating steady states are obtained

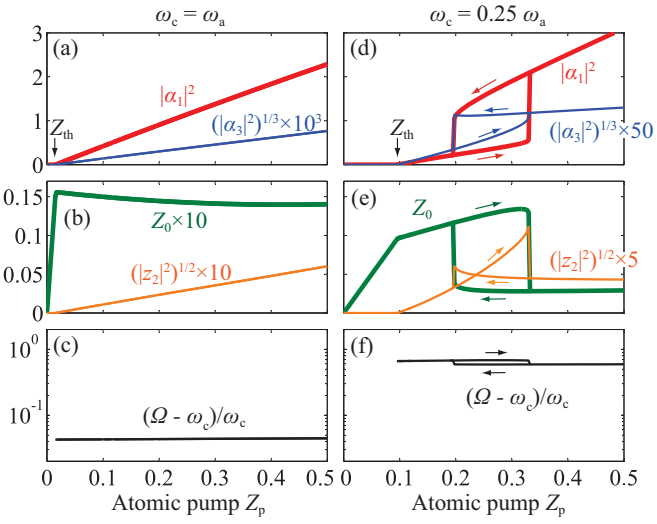

FIG. 1. Laser solutions are calculated by increasing and decreasing the atomic pump Z_p in the velocity form. The bare cavity frequencies are (a)–(c) $\omega_c = \omega_a$ and (d)–(f) $\omega_c = 0.25\omega_a$. (a) and (d) Intensities of fundamental component α_1 and the 3Ω one α_3 of the nondimensional vector potential $\mathcal{A} = \langle \hat{a} + \hat{a}^\dagger \rangle / \sqrt{N}$, (b) and (e) time-constant component Z_0 and the 2Ω one z_2 of the atomic population, and (c) and (f) $(\Omega - \omega_c)/\omega_c$ for fundamental oscillation frequency Ω are plotted. Below threshold $Z_p < Z_{th}$, we get $Z_0 = Z_p$ and zero oscillating components. Above threshold, we get a linear increase of $|\alpha_1|^2$, $|z_2| \propto |\alpha_1|^2$, and $|\alpha_3| = |\alpha_1|^3$ for $\omega_c = \omega_a$. A bistability appears for $\omega_c = 0.25\omega_a$. The arrows represent the solutions with increasing and decreasing Z_p. Parameters: $g' = 0.15$, $\gamma_\parallel = 0.05\omega_a$, $\gamma_{pure} = 0.1\omega_a$, and $\kappa = 0.01\omega_a$.

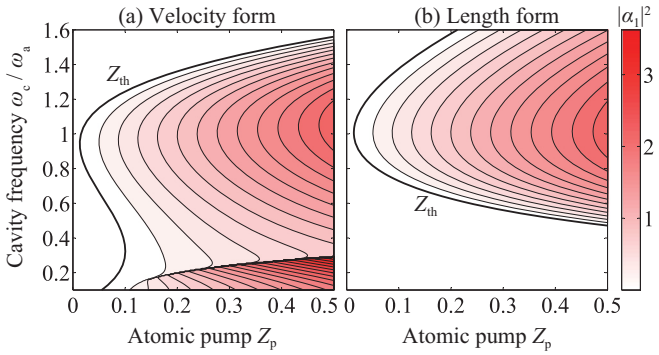

FIG. 2. Maps of laser solutions in (a) velocity form and (b) the length one. The intensity $|\alpha_1|^2$ of the fundamental component is calculated by increasing Z_p for a fixed ω_c, which is also changed in the vertical axis. The thick curves indicate the threshold Z_{th}. Unconventional solutions appear for low cavity frequency $\omega_c < 0.29\omega_a$ in the velocity form. Although we find only the conventional solutions in the length form under the current parameters, the unconventional solutions appear for larger g' or lower κ in Figs. 3 and 4. This quantitative difference is caused by the two-level and single-mode approximations used in the calculation. Parameters: $g' = 0.15$, $\gamma_\parallel = 0.05\omega_a$, $\gamma_{pure} = 0.1\omega_a$, and $\kappa = 0.01\omega_a$.

from Eqs. (4) and (5), and they correspond to the laser states. The detailed calculation is shown in Appendix B for the velocity form and in Appendix C for the length form.

In Fig. 1, we plot the laser solutions in the velocity form versus the atomic pump Z_p. The interaction strength is assumed to be $g' = 0.15$, which is relevant to the values reported for the organic molecules [15]. We suppose the atomic dissipation rates to be $\gamma_\parallel = 0.05\omega_a$ and $\gamma_{pure} = 0.1\omega_a$ by considering currently available samples. The supposed cavity loss rate $\kappa = 0.01\omega_a$ is lower than the one in Ref. [15], but a much lower rate is available from distributed Bragg reflectors [31–33]. In Figs. 1(a)–1(c), the bare cavity frequency is equal to the atomic one, $\omega_c = \omega_a$. Below the threshold $Z_{th} = 1.56 \times 10^{-2}$, the atomic population simply increases with obeying $Z = Z_0 = Z_p$, and the oscillation components are zero. Above the threshold, the intensity of the fundamental oscillation component increases linearly as $|\alpha_1|^2 \propto (Z_p - Z_{th})$, as seen in Fig. 1(a), and the time-constant component Z_0 of the atomic population is almost unchanged after the threshold as in Fig. 1(b). These are similar to the characteristics of the conventional laser.

The difference is the appearance of the multiple harmonics (z_2 and α_3), which are generally obtained even though higher cavity modes with $2\omega_c, 3\omega_c, \ldots$ are not considered [34]. As seen in Figs. 1(a) and 1(b), the multiple harmonics increase as $|z_2|^2 \propto (Z_p - Z_{th})^2$ and $|\alpha_3|^2 \propto (Z_p - Z_{th})^3$ which are similar to the characteristics of the third-order nonlinear effect (perturbation) with respect to the fundamental component α_1.

In contrast, in Figs. 1(d)–1(f), where the cavity frequency is far below the atomic resonance as $\omega_c = 0.25\omega_a$, we can find a bistable behavior above the threshold $Z_{th} = 9.62 \times 10^{-2}$ [35]. In Fig. 2(a), we plot the intensity $|\alpha_1|^2$ of the fundamental component calculated in the velocity form by increasing Z_p for a fixed ω_c, which is also changed in the vertical axis. When ω_c is around the atomic frequency ω_a, the threshold Z_{th} is minimized, and $|\alpha_1|^2$ is locally maximized. The bistability appears for low cavity frequency $0.15\omega_a < \omega_c < 0.29\omega_a$. For $\omega_c < 0.15\omega_a$, we do not find a clear jump, and the solutions change continuously (but drastically) with the increase of Z_p.

The appearance of the bistability can be understood simply by the fact that the third harmonic gets close to the atomic resonance [$3\Omega \sim 1.2\omega_a$ in Figs. 1(d)–1(f)]. Comparing with Fig. 1(a) ($3\Omega \sim 3.1\omega_a$), the 3Ω component α_3 is significantly enhanced in Fig. 1(d), while the fundamental one α_1 is of the same order. Thanks to the relatively large amplitudes of the multiple harmonics, we can find unconventional solutions for the complicated nonlinear equations (4) and (5) with the five variables (or more in the multiharmonic expansion). This is the reason why the bistability appears for the low cavity frequency in Fig. 2(a). To increase the ω_c range showing the laser down to such a low frequency, strong g', low κ, and high $\gamma_{total} = \gamma_\parallel + \gamma_{pure}$ are desired (for $\kappa < \gamma_{total}$), as expected from the conventional laser theory [3–6]. Further, a low pure-dephasing ratio $\gamma_{pure}/\gamma_{total}$ ($= 2/3$ in the present calculation) is advantageous to enhancing the multiharmonic amplitudes, and then the bistability appears more clearly. This tendency will be checked numerically in the next section.

The signature of the electromagnetic distinction appears particularly in the bistable region. In the resonant case ($\omega_c = \omega_a$), the interaction is suppressed effectively through

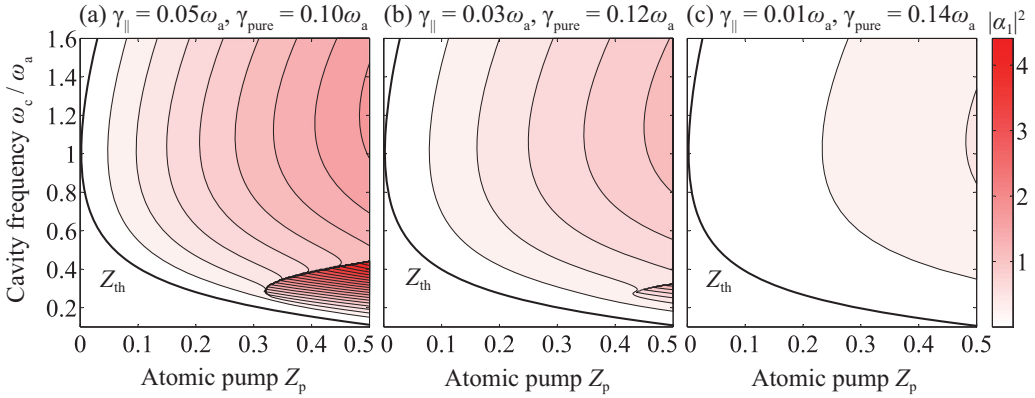

FIG. 3. Maps of laser solutions calculated in the length form for $g' = 0.4$ and $\kappa = 0.01\omega_a$. The atomic dissipation rates are shown above the plots. The unconventional solutions appear for strong enough interaction g' and low enough cavity loss κ even in the length form, while they disappear by increasing the ratio $\gamma_{pure}/\gamma_{total}$ while keeping the total dissipation rate $\gamma_{total} = \gamma_\parallel + \gamma_{pure}$.

$2g\omega_a\bar{\mathcal{A}}\bar{Z}$ in Eq. (4c) and $2g\omega_c\tilde{\Pi}\tilde{Z}$ in Eq. (5d) via the negligible atomic population $Z \sim 0.01$ shown in Fig. 1(b). Then, the laser is reduced approximately to the conventional one, and the multiple harmonics appear perturbatively. In this sense, the bistability in Figs. 1(d)–1(f) is correlated strongly to the electromagnetic distinction because the interaction is not significantly suppressed by the atomic population $Z \sim 0.1$, as seen in Fig. 1(e). The signature of the distinction is also found in Figs. 1(c) and 1(f), showing $(\Omega - \omega_c)/\omega_c = |p_1/\alpha_1| - 1$, i.e., the amplitude difference between the nondimensional vector potential and the electric field [this relation is obtained from Eq. (4a) in the velocity form]. The negligible difference $|p_1/\alpha_1| - 1 \ll 1$ in Fig. 1(c) corresponds approximately to the conventional laser, in which the photons are well defined as $|\alpha_1| = |p_1|$. In contrast, in the bistable case, the relatively large $|p_1/\alpha_1| - 1$ in Fig. 1(f) indicates that the electric field Π and the magnetic one (or vector potential $\mathcal{A}$) show clearly distinct dynamics including the multiple harmonics. This is certainly what we initially expected in the ultrastrong regime, and the bistability originates from this distinction [36].

IV. QUANTITATIVE INFLUENCES BY LEVEL AND MODE TRUNCATIONS

In Fig. 2(b), the laser solutions calculated in the length form are plotted under the same parameters as in Fig. 2(a). Although the bistability does not appear in Fig. 2(b), it is just the quantitative difference caused by the two-level and single-mode approximations, and we can obtain the bistability even in the length form for different parameters, as seen in Figs. 3 and 4. The maps of laser solutions in the length form are plotted in Fig. 3(a) for stronger electromagnetic interaction with matter $g' = 0.4$ and in Fig. 4(a) for lower cavity loss $\kappa = 0.001\omega_a$ compared with the parameters in Fig. 2. Under these conditions, the bistability appears even in the length form.

In Figs. 3–5, the dependence on the pure-dephasing rate γ_{pure} is also shown. Figures 3 and 4 are calculated in the length form, and Figs. 5 is calculated in the velocity form [Fig. 5(a) is equivalent to Fig. 2(a)]. The pure-dephasing ratio $\gamma_{pure}/\gamma_{total}$ is changed while keeping the total dissipation rates $\gamma_{total} = \gamma_\parallel + \gamma_{pure} = 0.15\omega_a$. In the conventional laser theory [6], the laser occurs under the following condition (determining the

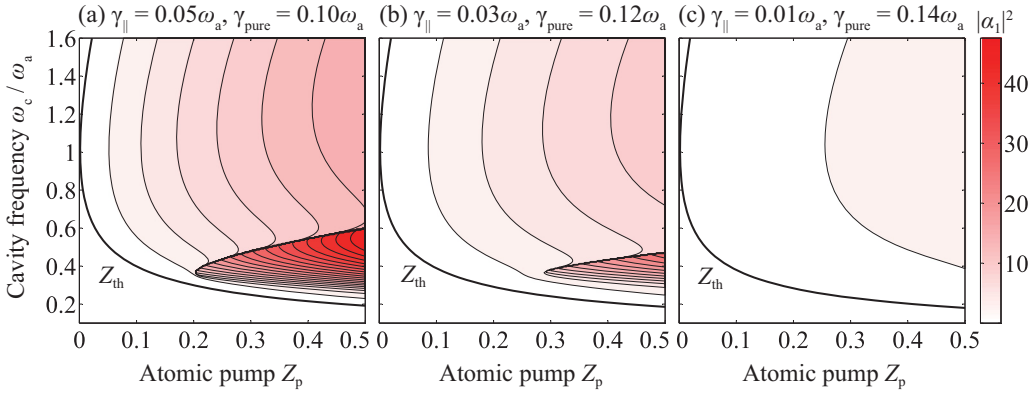

FIG. 4. Maps of laser solutions calculated in the length form for $g' = 0.15$ and $\kappa = 0.001\omega_a$. The atomic dissipation rates are shown above the plots. The unconventional solutions appear for strong enough interaction g' and low enough cavity loss κ even in the length form, while they disappear by increasing the ratio $\gamma_{pure}/\gamma_{total}$ with keeping the total dissipation rate $\gamma_{total} = \gamma_\parallel + \gamma_{pure}$.

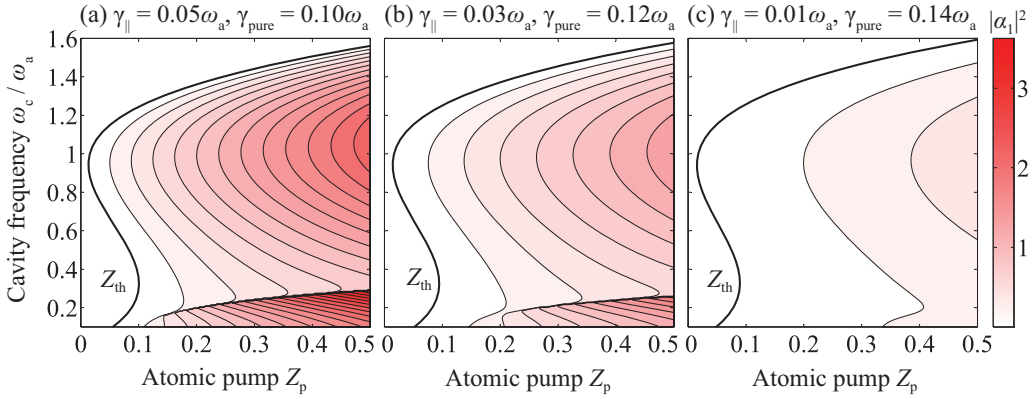

FIG. 5. Maps of laser solutions calculated in the velocity form for $g' = 0.15$ and $\kappa = 0.01\omega_a$. The atomic dissipation rates are shown above the plots [(a) is equivalent to Fig. 2(a)].

threshold Z_{th}):

$$\frac{2g^2\omega_a^2 Z_p}{\kappa\gamma_{total} - (\omega_c - \Omega)(\omega_a - \Omega)} > 1, \tag{6}$$

where the oscillation frequency is obtained as

$$\Omega = \frac{\kappa\omega_a + \gamma_{total}\omega_c}{\kappa + \gamma_{total}}. \tag{7}$$

In this way, the ω_c range showing the conventional laser does not depend on the pure-dephasing ratio $\gamma_{pure}/\gamma_{total}$, and this tendency basically survives even in Figs. 3–5. Equation (6) is rewritten as

$$2g^2\omega_a^2 Z_p > \kappa\gamma_{total}\left[1 + \left(\frac{\omega_a - \omega_c}{\gamma_{total} + \kappa}\right)^2\right]. \tag{8}$$

This relation basically determines the ω_c range of the laser. Since we suppose $\kappa \ll \gamma_{total}$, the ω_c range is enlarged by lowering κ and by heightening γ_{total} and g'.

In the calculations in Figs. 3–5, the bistable laser solutions are obtained for $\omega_c \sim \omega_a/3$, which is the requirement for the bistability, as discussed in the previous section. However, by increasing the pure-dephasing ratio $\gamma_{pure}/\gamma_{total}$, the unconventional solutions gradually disappear. This is because the amplitudes of the electromagnetic fields are diminished, as clearly seen in the figures. Especially, the third-harmonic amplitudes are diminished more drastically (not shown in the figures) because they appear to be similar to the nonlinear optical effect. For much lower $\gamma_{pure}/\gamma_{total}$, the bistability appears more clearly (not shown in the figures). Then, to obtain the bistability, we should prepare low enough κ and γ_{pure} and high enough $\gamma_\parallel$ and g'.

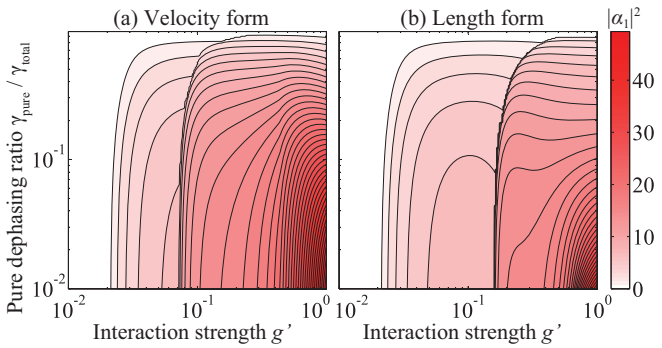

FIG. 6. Maps of laser solutions in (a) velocity form and (b) the length one. The color indicates the maximum $|\alpha_1|^2$ found by changing ω_c. The larger value is chosen in the bistable case. The maximum $|\alpha_1|^2$ is plotted versus the interaction strength g' and the pure-dephasing ratio $\gamma_{pure}/\gamma_{total}$ with keeping $Z_p = 0.5$, $\gamma_{total} = 0.15\omega_a$, and $\kappa = 0.01\omega_a$.

In Fig. 6, we plot the maximum $|\alpha_1|^2$ found by changing ω_c in the two forms of the light-matter interaction. The larger $|\alpha_1|^2$ is chosen in the bistable case, and it is plotted versus the interaction strength g' and the pure-dephasing ratio $\gamma_{pure}/\gamma_{total}$ while keeping $Z_p = 0.5$, $\gamma_{total} = 0.15\omega_a$, and $\kappa = 0.01\omega_a$. The relatively large $|\alpha_1|^2$ for strong enough g' indicates the existence of the bistability. In both forms, whereas the bistability is obtained clearly for low enough $\gamma_{pure}/\gamma_{total}$, the visibility is lowered with the increase in $\gamma_{pure}/\gamma_{total}$. This tendency indicates the disappearance of the bistability demonstrated in Figs. 3–5. Whereas the bistability is obtained even for the relatively high $\gamma_{pure}/\gamma_{total} \sim 0.8$, as shown in Figs. 3–5, strong enough g' is required for the bistability, as seen in Fig. 6. The bistable region is not largely enhanced even in the limit of $\gamma_{pure}/\gamma_{total} \to 0$. This is because the pure-dephasing ratio $\gamma_{pure}/\gamma_{total}$ basically does not change the parameter region showing $\Omega \sim \omega_a/3$, which is determined by Eq. (8).

In Fig. 7, the parameter regions showing the bistability calculated in the two forms are plotted. We plot Z_0 in the steady state for the highest bare-cavity frequency that shows the bistability for $Z_p = 0.5$ [$\omega_c = 0.29\omega_a$ in Fig. 2(a)] as functions of g' and κ. The bistability appears basically for strong enough g' and low enough κ/ω_a, both of which are necessary for obtaining the laser around $3\Omega \sim \omega_a$, as discussed above. The population Z_0 is a measure of the electromagnetic distinction. The bistability starts to appear with a large Z_0, which enhances the distinction of the electromagnetic fields, and Z_0 still keeps a certain value ($\sim$0.06 at current parameters) even when the bistability is easily found for large enough g'.

The quantitative difference for the appearance of the bistability mathematically originates from the following fact.

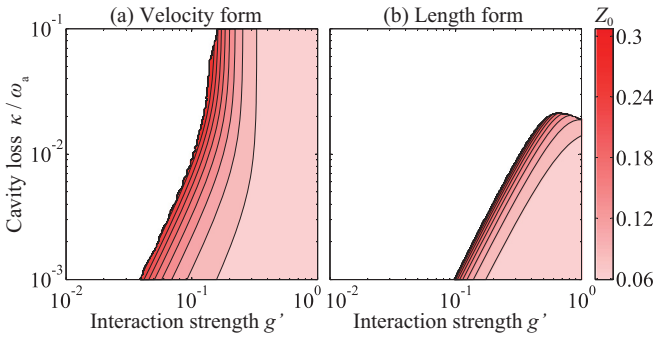

FIG. 7. The region of parameters g' and κ/ω_a showing the bistability is plotted in (a) velocity form and (b) the length one. The color indicates Z_0 (a measure of electromagnetic distinction) for the highest bare cavity frequency that shows the bistability at $Z_p = 0.5$. In both forms, the bistability appears for strong enough interaction g' and low enough cavity loss κ. Parameters: $\gamma_\parallel = 0.05\omega_a$ and $\gamma_{pure} = 0.1\omega_a$.

As seen in Eqs. (1) and (2), the interaction terms are proportional to $g\omega_a$ and $g\omega_c$ in the velocity and length forms, respectively. Since the coefficient $g\omega_a \propto 1/\sqrt{\omega_c}$ is increased with the decrease of ω_c in the velocity form, the laser solution is easily found for low ω_c. As a result, the bistability is easily found in the velocity form compared to the length one. Although this quantitative form dependence is diminished if we consider all the atomic levels and the cavity modes by specifying particular systems of interest [19,20,37], the two-level approximation is justified qualitatively if the two atomic levels are well separated by more than $g\omega_a$ or $g\omega_c$ from the other levels energetically [38]. Since the higher cavity modes basically enhance the amplitudes of the multiple harmonics, the bistability (or multistability) is also expected beyond the single-mode approximations [39]. Whereas the present calculation still has such quantitative problems, the bistability is expected to appear as another qualitative difference from the conventional laser.

V. SUMMARY

We conclude that, in the ultrastrong regime, the laser generally accompanies odd-order harmonics of the electromagnetic fields both inside and outside the cavity and the synchronization with the atomic population oscillating with even-order harmonics. Whereas we found a bistability via the calculation up to the third harmonic under the two-level and single-mode approximations, a richer variety of the laser solutions could be obtained thanks to the recovery of the original distinction of the electromagnetic fields in the ultrastrong regime, which exposes the additional degrees of freedom hidden by the RWA. However, since we investigated the laser dynamics under the two-level and single-mode approximations, we got quantitatively different results in the velocity and length forms of the light-matter interaction, whereas the multiple harmonics and the bistability are reliable qualitatively. In order to eliminate this quantitative problem of the form choice, we must discuss which form is appropriate in the finite-level and finite-mode approximation in the future.

The properties of this laser are not fully elucidated in this paper, and those to be investigated spread as extensively as the conventional laser has been studied from the viewpoints of quantum optics, nonlinear physics, nonequilibrium physics, synergetics, etc. For example, it is open to dispute whether the laser output is in a simple coherent state like the ideal conventional laser [3–6] or a nonclassical state can be directly obtained thanks to the ultrastrong interaction, especially in the bistable regions [40]. Experimentally, the laser in the ultrastrong regime would be realized by fabricating microcavities embedding organic (dye) molecules [15] or superconducting circuits [43] with (a large number of) artificial atoms. Quantum cascade lasers involving intersubband transitions in semiconductor quantum wells [8–11,16] are also promising, while the present calculation does not exactly correspond to the quantum cascade lasers.

ACKNOWLEDGMENTS

M.B. thanks H. Ishihara for discussion. This work was funded by the ImPACT Program of the Council for Science, Technology and Innovation (Cabinet Office, government of Japan) and by JSPS KAKENHI (Grants No. 26287087 and No. 24-632).

APPENDIX A: STOCHASTIC DIFFERENTIAL EQUATIONS

As a general discussion, we consider system-environment coupling expressed as

$$\hat{H}_{SEC}^{example} = \int_0^\infty d\omega \left\{ \hbar\omega \hat{f}^\dagger(\omega)\hat{f}(\omega) + i\hbar\sqrt{\frac{\Gamma}{2\pi}}\hat{S}[\hat{f}^\dagger(\omega) - \hat{f}(\omega)] \right\}. \tag{A1}$$

Here, $\hat{S}$ is a Hermitian operator of the system of interest, and $\hat{f}(\omega)$ is the annihilation operator of a boson with a frequency ω in the environment. Γ corresponds to the bare dissipation rate. Further, the distribution in the environment is supposed as

$$\langle \hat{f}^\dagger(\omega)\hat{f}(\omega')\rangle = n\delta(\omega - \omega'), \tag{A2a}$$

$$\langle \hat{f}(\omega)\hat{f}^\dagger(\omega')\rangle = (n+1)\delta(\omega - \omega'), \tag{A2b}$$

where n is the expectation number of bosons in the environment. From this Hamiltonian for frequency-independent dissipation rate Γ and flat distribution n, without applying the RWA to the system-environment coupling, the quantum stochastic differential equation (QSDE) is obtained for system operator $\hat{O}$ in Itoh's form as [6,26]

$$\begin{aligned} d\hat{O} = {} & \frac{1}{i\hbar}[\hat{O},\hat{H}_0]dt + \frac{\Gamma n}{2}\{\hat{S}^{(+)}[\hat{O},\hat{S}] + [\hat{S},\hat{O}]\hat{S}^{(-)}\}dt \\ & + \frac{\Gamma(n+1)}{2}\{\hat{S}^{(-)}[\hat{O},\hat{S}] + [\hat{S},\hat{O}]\hat{S}^{(+)}\}dt \\ & - \sqrt{\Gamma}\{[\hat{O},\hat{S}]d\hat{F}(t) + d\hat{F}^\dagger(t)[\hat{S},\hat{O}]\}, \end{aligned} \tag{A3}$$

where the fluctuation operator satisfies

$$d\hat{F}(t)^2 = d\hat{F}^\dagger(t)^2 = 0, \tag{A4a}$$

$$d\hat{F}^\dagger(t)d\hat{F}(t) = ndt, \tag{A4b}$$

$$d\hat{F}(t)d\hat{F}^\dagger(t) = (n+1)dt. \tag{A4c}$$

When we replace $\hat{S}$ by $\hat{S}^{(+)}$ or $\hat{S}^{(-)}$, Eq. (A3) is certainly reduced to the QSDE discussed in Ref. [6]. Since Eq. (A3) only has the commutator between $\hat{O}$ and the original Hermitian operator $\hat{S}$, we do not need knowledge of the eigenstates of $\hat{H}_0$, which is generally hard to calculate.

For the dissipation and incoherent pumping (by a heat bath with a negative temperature [6]) of the laser system, we consider the following system-environment couplings:

$$\begin{aligned}\hat{H}^x_{\rm SEC} = \int_0^\infty d\omega \Big\{ & \hbar\omega \hat{f}^\dagger_A(\omega)\hat{f}_A(\omega) + \hbar\omega \sum_{\lambda=1}^{N} [\hat{f}^\dagger_{X,\lambda}(\omega)\hat{f}_{X,\lambda}(\omega) \\ & + \hat{f}^\dagger_{Z,\lambda}(\omega)\hat{f}_{Z,\lambda}(\omega)] \\ & + i\hbar\sqrt{\frac{\kappa}{2\pi}}(\hat{a}+\hat{a}^\dagger)[\hat{f}^\dagger_A(\omega) - \hat{f}_A(\omega)] \\ & + i\hbar\sqrt{\frac{\gamma_\parallel |Z_{\rm p}|}{\pi}} \sum_{\lambda=1}^{N} \hat{\sigma}^x_\lambda [\hat{f}^\dagger_{X,\lambda}(\omega) - \hat{f}_{X,\lambda}(\omega)] \\ & + i\hbar\sqrt{\frac{\gamma_{\rm pure}}{4\pi}} \sum_{\lambda=1}^{N} \hat{\sigma}^z_\lambda [\hat{f}^\dagger_{Z,\lambda}(\omega) - \hat{f}_{Z,\lambda}(\omega)] \Big\}. \end{aligned} \tag{A5}$$

The fields $\hat{f}_A(\omega)$, $\hat{f}_{X,\lambda}(\omega)$, and $\hat{f}_{Z,\lambda}(\omega)$ in the environments are not correlated with each other, and their self-correlations are supposed as

$$\langle \hat{f}^\dagger_A(\omega)\hat{f}_A(\omega')\rangle = 0, \tag{A6a}$$

$$\langle \hat{f}_A(\omega)\hat{f}^\dagger_A(\omega')\rangle = \delta(\omega-\omega'), \tag{A6b}$$

$$\langle \hat{f}^\dagger_{X,\lambda}(\omega)\hat{f}_{X,\lambda'}(\omega')\rangle = \frac{1/2+Z_{\rm p}}{2|Z_{\rm p}|}\delta_{\lambda,\lambda'}\delta(\omega-\omega'), \tag{A7a}$$

$$\langle \hat{f}_{X,\lambda}(\omega)\hat{f}^\dagger_{X,\lambda'}(\omega')\rangle = \frac{1/2-Z_{\rm p}}{2|Z_{\rm p}|}\delta_{\lambda,\lambda'}\delta(\omega-\omega'), \tag{A7b}$$

$$\langle \hat{f}^\dagger_{Z,\lambda}(\omega)\hat{f}_{Z,\lambda'}(\omega')\rangle = 0, \tag{A8a}$$

$$\langle \hat{f}_{Z,\lambda}(\omega)\hat{f}^\dagger_{Z,\lambda'}(\omega')\rangle = \delta_{\lambda,\lambda'}\delta(\omega-\omega'). \tag{A8b}$$

From these system-environment couplings, the equations of motion of the c-number variables in the main text are derived from Eq. (A3). For the derivation, we considered that the following term is approximately zero:

$$\langle \hat{\sigma}^{x(+)}_\lambda \hat{\sigma}^z_\lambda + \hat{\sigma}^z_\lambda \hat{\sigma}^{x(+)}_\lambda \rangle - \langle \hat{\sigma}^{x(-)}_\lambda \hat{\sigma}^z_\lambda + \hat{\sigma}^z_\lambda \hat{\sigma}^{x(-)}_\lambda \rangle \simeq 0. \tag{A9}$$

To derive this, from the relations $\hat{\sigma}^x_\lambda = \hat{\sigma}^{x(+)}_\lambda + \hat{\sigma}^{x(-)}_\lambda$ and $\hat{\sigma}^z_\lambda \hat{\sigma}^x_\lambda = i\hat{\sigma}^y_\lambda$, we get the following relation:

$$\langle \hat{\sigma}^{x(+)}_\lambda \hat{\sigma}^z_\lambda + \hat{\sigma}^z_\lambda \hat{\sigma}^{x(+)}_\lambda \rangle = -\langle \hat{\sigma}^{x(-)}_\lambda \hat{\sigma}^z_\lambda + \hat{\sigma}^z_\lambda \hat{\sigma}^{x(-)}_\lambda \rangle. \tag{A10}$$

The left- and right-hand sides oscillate mainly with positive and negative frequencies, respectively. Then, to satisfy Eq. (A10), both brackets should be zero, and Eq. (A9) can be neglected. Further, we used the following approximation:

$$-\sum_{\lambda=1}^{N} \frac{\langle \hat{\sigma}^{x(+)}_\lambda \hat{\sigma}^y_\lambda \rangle + \langle \hat{\sigma}^y_\lambda \hat{\sigma}^{x(+)}_\lambda \rangle}{iN} \simeq 1. \tag{A11}$$

The pumping level $Z_{\rm p}$ is modulated by this factor in the equations of motion in Eqs. (4) and (5). When the RWA can be applied to the electromagnetic interaction with matter in the photon-excitation basis, we get $\hat{\sigma}^{x(+)}_\lambda = \hat{\sigma}_\lambda$ and $\hat{\sigma}^{y(+)}_\lambda = i\hat{\sigma}_\lambda$; then we can get the above equality. In the ultrastrong regime, the equality is generally violated. However, if we get $|Z| \ll 1$, the strength of the interaction is effectively suppressed, and $\hat{\sigma}^{x(+)}_\lambda \simeq \hat{\sigma}_\lambda$ and $\hat{\sigma}^{y(+)}_\lambda \simeq i\hat{\sigma}_\lambda$ are also obtained approximately. Even if $|Z|$ is not negligible, the atomic pump $Z_{\rm p}$ multiplied by Eq. (A11) shows the even-order harmonics. Further, for large enough $N \gg 1$, the deviation from unity can be neglected like the products of the operators are factorized under the mean-field approximation in the macroscopic laser equation.

APPENDIX B: OSCILLATING STEADY STATES IN THE VELOCITY FORM

We decompose the five variables to frequency components as $\mathcal{A}(t) = \alpha_1 e^{-i\Omega t} + \alpha_3 e^{-i3\Omega t} + \text{c.c.}$ (Π to p_n, X to x_n, and Y to y_n), and $Z(t) = Z_0 + (z_2 e^{-i2\Omega t} + \text{c.c.})$. Then, neglecting highly oscillating terms, the equations of the frequency components are obtained in the velocity form as

$$(\partial/\partial t)\bar{\alpha}_n = in\Omega\bar{\alpha}_n - \omega_{\rm c}\bar{p}_n, \tag{B1a}$$

$$(\partial/\partial t)\bar{p}_n = (\omega_{\rm c} + 4g^2\omega_{\rm a} - i\kappa)\bar{\alpha}_n + in\Omega\,\bar{p}_n + 4g\omega_{\rm a}\bar{y}_n, \tag{B1b}$$

$$\begin{aligned}(\partial/\partial t)\bar{x}_1 = {} & (i\Omega - \gamma_x)\bar{x}_1 - \omega_{\rm a}\bar{y}_1 \\ & + 2g\omega_{\rm a}(\bar{Z}_0\bar{\alpha}_1 + \bar{z}^*_2\bar{\alpha}_3 + \bar{\alpha}^*_1\bar{z}_2),\end{aligned} \tag{B1c}$$

$$\begin{aligned}(\partial/\partial t)\bar{x}_3 = {} & (i3\Omega - \gamma_x)\bar{x}_3 - \omega_{\rm a}\bar{y}_3 \\ & + 2g\omega_{\rm a}(\bar{Z}_0\bar{\alpha}_3 + \bar{\alpha}_1\bar{z}_2),\end{aligned} \tag{B1d}$$

$$(\partial/\partial t)\bar{y}_n = \omega_{\rm a}\bar{x}_n + (in\Omega - \gamma_y)\bar{y}_n, \tag{B1e}$$

$$(\partial/\partial t)\bar{Z}_0 = -\gamma_z\big(\bar{Z}_0 - Z_{\rm p}\big) - 2g\omega_{\rm a}(\bar{\alpha}^*_1\bar{x}_1 + \bar{\alpha}^*_3\bar{x}_3 + \text{c.c.}), \tag{B1f}$$

$$(\partial/\partial t)\bar{z}_2 = (i2\Omega - \gamma_z)\bar{z}_2 - 2g\omega_{\rm a}(\bar{\alpha}^*_1\bar{x}_3 + \bar{\alpha}_1\bar{x}_1 + \bar{x}^*_1\bar{\alpha}_3). \tag{B1g}$$

In oscillating steady states, all of these derivatives should be zero. Equations to be satisfied are finally reduced to

$$\begin{aligned}0 = \Big\{ & \frac{\Delta_{c,1}\Delta_{a,1}}{8g^2\omega_{\rm c}\omega^3_{\rm a}} + Z_{\rm p} \\ & + [C_{|1|^2 1} + C_{|3|^2 1}|\eta|^2 + C_{(-1)^2 3}\eta]|\bar{\alpha}_1|^2 \Big\}\bar{\alpha}_1,\end{aligned} \tag{B2a}$$

$$\begin{aligned}0 = \Big\{ & \frac{\Delta_{c,3}\Delta_{a,3}}{8g^2\omega_{\rm c}\omega^3_{\rm a}} + Z_{\rm p} \\ & + [C_{|1|^2 3} + C_{|3|^2 3}|\eta|^2 + C_{1^3}\eta^{-1}]|\bar{\alpha}_1|^2 \Big\}\eta\bar{\alpha}_1 e^{i2\theta},\end{aligned} \tag{B2b}$$

where θ is the phase of $\bar{\alpha}_1 = |\bar{\alpha}_1|e^{i\theta}$. Unknown variables are Ω, $|\bar{\alpha}_1| \in \mathbb{R}$, and a complex value

$$\eta = \frac{\bar{\alpha}_3}{\bar{\alpha}_1}e^{-i2\theta} \in \mathbb{C}. \tag{B3}$$

The other quantities in Eqs. (B2) are defined as follows:

$$\Delta_{c,n} = \omega_c(\omega_c + 4g^2\omega_a) - n^2\Omega^2 - i\kappa\omega_c, \tag{B4a}$$
$$\Delta_{a,n} = {\omega_a}^2 + (in\Omega - \gamma_x)(in\Omega - \gamma_y), \tag{B4b}$$

$$C_{|1|^21} = -\frac{\mathrm{Re}[(i\Omega - \gamma_y)\Delta_{c,1}]}{\gamma_z\omega_c\omega_a} + \frac{(i\Omega - \gamma_y)\Delta_{c,1}}{2\omega_c\omega_a(i2\Omega - \gamma_z)}, \tag{B5a}$$

$$C_{|3|^21} = -\frac{\mathrm{Re}[(i3\Omega - \gamma_y)\Delta_{c,3}]}{\gamma_z\omega_c\omega_a} + \frac{(i3\Omega + \gamma_y)\Delta^*_{c,3} - (i\Omega - \gamma_y)\Delta_{c,1}}{2\omega_c\omega_a(i2\Omega + \gamma_z)}, \tag{B5b}$$

$$C_{(-1)^23} = \frac{(i3\Omega - \gamma_y)\Delta_{c,3} - (i\Omega + \gamma_y)\Delta^*_{c,1}}{2\omega_c\omega_a(i2\Omega - \gamma_z)} + \frac{(i\Omega + \gamma_y)\Delta^*_{c,1}}{2\omega_c\omega_a(i2\Omega + \gamma_z)}, \tag{B5c}$$

$$C_{|1|^23} = -\frac{\mathrm{Re}[(i\Omega - \gamma_y)\Delta_{c,1}]}{\gamma_z\omega_c\omega_a} + \frac{(i3\Omega - \gamma_y)\Delta_{c,3} - (i\Omega + \gamma_y)\Delta^*_{c,1}}{2\omega_c\omega_a(i2\Omega - \gamma_z)}, \tag{B5d}$$

$$C_{|3|^23} = -\frac{\mathrm{Re}[(i3\Omega - \gamma_y)\Delta_{c,3}]}{\gamma_z\omega_c\omega_a}, \tag{B5e}$$

$$C_{1^3} = \frac{(i\Omega - \gamma_y)\Delta_{c,1}}{2\omega_c\omega_a(i2\Omega - \gamma_z)}. \tag{B5f}$$

Once we get a solution to Eqs. (B2), the other frequency components are obtained as

$$\bar{\alpha}_3 = \eta\bar{\alpha}_1 e^{i2\theta}, \tag{B6a}$$
$$\bar{p}_n = \frac{in\Omega}{\omega_c}\bar{\alpha}_n, \tag{B6b}$$
$$\bar{x}_n = \frac{(in\Omega - \gamma_y)\Delta_{c,n}}{4g\omega_c\omega_a^2}\bar{\alpha}_n, \tag{B6c}$$
$$\bar{y}_n = -\frac{\omega_a}{in\Omega - \gamma_y}\bar{x}_n, \tag{B6d}$$
$$\bar{Z}_0 = Z_p - \frac{2g\omega_a}{\gamma_z}(\bar{\alpha}^*_1\bar{x}_1 + \bar{\alpha}^*_3\bar{x}_3 + \mathrm{c.c.}), \tag{B6e}$$
$$\bar{z}_2 = \frac{2g\omega_a}{(i2\Omega - \gamma_z)}(\bar{\alpha}^*_1\bar{x}_3 + \bar{\alpha}_1\bar{x}_1 + \bar{x}^*_1\bar{\alpha}_3), \tag{B6f}$$

while the phase θ of $\bar{\alpha}_1$ can be chosen arbitrarily.

APPENDIX C: OSCILLATING STEADY STATES IN THE LENGTH FORM

In the same manner as in the velocity form, the equations of the frequency components are obtained in the length form as

$$(\partial/\partial t)\tilde{\alpha}_n = in\Omega\tilde{\alpha}_n - \omega_c\tilde{p}_n + 4g\omega_c\tilde{x}_n, \tag{C1a}$$
$$(\partial/\partial t)\tilde{p}_n = (\omega_c - i\kappa)\tilde{\alpha}_n + in\Omega\tilde{p}_n, \tag{C1b}$$
$$(\partial/\partial t)\tilde{x}_n = (in\Omega - \gamma_x)\tilde{x}_n - \omega_a\tilde{y}_n, \tag{C1c}$$
$$(\partial/\partial t)\tilde{y}_1 = \omega_a\tilde{x}_1 + (i\Omega - \gamma_y)\tilde{y}_1 - 8g^2\omega_c(\tilde{Z}_0\tilde{x}_1 + \tilde{z}^*_2\tilde{x}_3 + \tilde{x}^*_1\tilde{z}_2) + 2g\omega_c(\tilde{Z}_0\tilde{p}_1 + \tilde{z}^*_2\tilde{p}_3 + \tilde{p}^*_1\tilde{z}_2), \tag{C1d}$$
$$(\partial/\partial t)\tilde{y}_3 = \omega_a\tilde{x}_3 + (i3\Omega - \gamma_y)\tilde{y}_3 - 8g^2\omega_c(\tilde{Z}_0\tilde{x}_3 + \tilde{x}_1\tilde{z}_2) + 2g\omega_c(\tilde{Z}_0\tilde{p}_3 + \tilde{p}_1\tilde{z}_2), \tag{C1e}$$
$$(\partial/\partial t)\tilde{Z}_0 = -\gamma_z(\tilde{Z}_0 - Z_p) + 8g^2\omega_c(\tilde{x}^*_1\tilde{y}_1 + \tilde{x}^*_3\tilde{y}_3 + \mathrm{c.c.}) - 2g\omega_c(\tilde{p}^*_1\tilde{y}_1 + \tilde{p}^*_3\tilde{y}_3 + \mathrm{c.c.}), \tag{C1f}$$
$$(\partial/\partial t)\tilde{z}_2 = (i2\Omega - \gamma_z)\tilde{z}_2 + 8g^2\omega_c(\tilde{x}^*_1\tilde{y}_3 + \tilde{x}_1\tilde{y}_1 + \tilde{y}^*_1\tilde{x}_3) - 2g\omega_c(\tilde{p}^*_1\tilde{y}_3 + \tilde{p}_1\tilde{y}_1 + \tilde{y}^*_1\tilde{p}_3). \tag{C1g}$$

The equations to solve are

$$0 = \left\{\frac{\Delta_{c,1}\Delta_{a,1}}{8g^2\omega_c\omega_a\Omega^2} + Z_p + [C_{|1|^21} + C_{|3|^21}|\eta|^2 + C_{(-1)^23}\eta]|\tilde{\alpha}_1|^2\right\}\tilde{\alpha}_1, \tag{C2a}$$

$$0 = \left\{\frac{\Delta_{c,3}\Delta_{a,3}}{8g^2\omega_c\omega_a\Omega^2} + 9Z_p + [C_{|1|^23} + C_{|3|^23}|\eta|^2 + C_{1^3}\eta^{-1}]|\tilde{\alpha}_1|^2\right\}\eta\tilde{\alpha}_1 e^{i2\theta} \tag{C2b}$$

for unknown variables Ω, $|\tilde{\alpha}_1| \in \mathbb{R}$, and $\eta = e^{-i2\theta}\tilde{\alpha}_3/\tilde{\alpha}_1 \in \mathbb{C}$. The other quantities in Eqs. (C2) are defined as follows:

$$\Delta_{c,n} = {\omega_c}^2 - n^2\Omega^2 - i\kappa\omega_c, \tag{C3a}$$
$$\Delta_{a,n} = {\omega_a}^2 + (in\Omega - \gamma_x)(in\Omega - \gamma_y), \tag{C3b}$$

$$C_{|1|^21} = -\frac{\mathrm{Re}[(i\Omega - \gamma_x)\Delta_{c,1}]}{\gamma_z\omega_c\omega_a} + \frac{(i\Omega - \gamma_x)\Delta_{c,1}}{2\omega_c\omega_a(i2\Omega - \gamma_z)}, \tag{C4a}$$

$$C_{|3|^21} = -\frac{\mathrm{Re}[(i3\Omega - \gamma_x)\Delta_{c,3}]}{\gamma_z\omega_c\omega_a} + \frac{(i3\Omega + \gamma_x)\Delta^*_{c,3} - 9(i\Omega - \gamma_x)\Delta_{c,1}}{2\omega_c\omega_a(i2\Omega + \gamma_z)}, \tag{C4b}$$

$$C_{(-1)^23} = -\frac{(i3\Omega - \gamma_x)\Delta_{c,3} - 9(i\Omega + \gamma_y)\Delta^*_{c,1}}{6\omega_c\omega_a(i2\Omega - \gamma_z)} - \frac{3(i\Omega + \gamma_x)\Delta^*_{c,1}}{2\omega_c\omega_a(i2\Omega + \gamma_z)}, \tag{C4c}$$

$$C_{|1|^23} = -\frac{9\mathrm{Re}[(i\Omega - \gamma_x)\Delta_{c,1}]}{\gamma_z\omega_c\omega_a} + \frac{(i3\Omega - \gamma_x)\Delta_{c,3} - 9(i\Omega + \gamma_x)\Delta^*_{c,1}}{2\omega_c\omega_a(i2\Omega - \gamma_z)}, \tag{C4d}$$

$$C_{|3|^23} = -\frac{9\mathrm{Re}[(i3\Omega - \gamma_x)\Delta_{c,3}]}{\gamma_z\omega_c\omega_a}, \tag{C4e}$$

$$C_{1^3} = -\frac{3(i\Omega - \gamma_x)\Delta_{c,1}}{2\omega_c\omega_a(i2\Omega - \gamma_z)}. \tag{C4f}$$

The other frequency components are obtained as

$$\tilde{\alpha}_3 = \eta\tilde{\alpha}_1 e^{i2\theta}, \tag{C5a}$$

$$\tilde{p}_n = -\frac{\omega_c - i\kappa}{in\Omega}\tilde{\alpha}_n, \tag{C5b}$$

$$\tilde{y}_n = -\frac{(in\Omega - \gamma_x)\Delta_{c,n}}{i4ng\omega_c\omega_a\Omega}\tilde{\alpha}_n, \tag{C5c}$$

$$\tilde{x}_n = \frac{\omega_a}{in\Omega - \gamma_x}\tilde{y}_n, \tag{C5d}$$

$$\tilde{Z}_0 = Z_p + \frac{i2g\Omega}{\gamma_z}(\tilde{\alpha}_1^*\tilde{y}_1 + 3\tilde{\alpha}_3^*\tilde{y}_3 - \text{c.c.}), \tag{C5e}$$

$$\tilde{z}_2 = -\frac{i2g\Omega}{i2\Omega - \gamma_z}(\tilde{\alpha}_1^*\tilde{y}_3 - \tilde{\alpha}_1\tilde{y}_1 - 3\tilde{y}_1^*\tilde{\alpha}_3). \tag{C5f}$$

[1] T. H. Maiman, Nature (London) **187**, 493 (1960).
[2] A. Schawlow and C. Townes, Phys. Rev. **112**, 1940 (1958).
[3] H. Haken, *Light and Matter lc/Licht und Materie Ic*, Optik/Optics, Vol. 5/25/2/2c (Springer, Berlin, 1970).
[4] H. Haken, *Light*, Vol. 2, *Laser Light Dynamics* (North Holland, Amsterdam, 1985).
[5] M. O. Scully and M. S. Zubairy, *Quantum Optics* (Cambridge University Press, Cambridge, 1997).
[6] C. W. Gardiner and P. Zoller, *Quantum Noise*, 3rd ed. (Springer, Berlin, 2004).
[7] C. Ciuti, G. Bastard, and I. Carusotto, Phys. Rev. B **72**, 115303 (2005).
[8] G. Gunter, A. A. Anappara, J. Hees, A. Sell, G. Biasiol, L. Sorba, S. De Liberato, C. Ciuti, A. Tredicucci, A. Leitenstorfer, and R. Huber, Nature (London) **458**, 178 (2009).
[9] A. A. Anappara, S. De Liberato, A. Tredicucci, C. Ciuti, G. Biasiol, L. Sorba, and F. Beltram, Phys. Rev. B **79**, 201303 (2009).
[10] Y. Todorov, A. M. Andrews, I. Sagnes, R. Colombelli, P. Klang, G. Strasser, and C. Sirtori, Phys. Rev. Lett. **102**, 186402 (2009).
[11] Y. Todorov, A. M. Andrews, R. Colombelli, S. De Liberato, C. Ciuti, P. Klang, G. Strasser, and C. Sirtori, Phys. Rev. Lett. **105**, 196402 (2010).
[12] T. Niemczyk, F. Deppe, H. Huebl, E. P. Menzel, F. Hocke, M. J. Schwarz, J. J. Garcia-Ripoll, D. Zueco, T. Hummer, E. Solano, A. Marx, and R. Gross, Nat. Phys. **6**, 772 (2010).
[13] A. Fedorov, A. K. Feofanov, P. Macha, P. Forn-Díaz, C. J. P. M. Harmans, and J. E. Mooij, Phys. Rev. Lett. **105**, 060503 (2010).
[14] P. Forn-Díaz, J. Lisenfeld, D. Marcos, J. J. García-Ripoll, E. Solano, C. J. P. M. Harmans, and J. E. Mooij, Phys. Rev. Lett. **105**, 237001 (2010).
[15] T. Schwartz, J. A. Hutchison, C. Genet, and T. W. Ebbesen, Phys. Rev. Lett. **106**, 196405 (2011).
[16] M. Porer, J.-M. Ménard, A. Leitenstorfer, R. Huber, R. Degl'Innocenti, S. Zanotto, G. Biasiol, L. Sorba, and A. Tredicucci, Phys. Rev. B **85**, 081302(R) (2012).
[17] G. Scalari, C. Maissen, D. Turčinková, D. Hagenmüller, S. De Liberato, C. Ciuti, C. Reichl, D. Schuh, W. Wegscheider, M. Beck, and J. Faist, Science **335**, 1323 (2012).
[18] Q. Zhang, T. Arikawa, E. Kato, J. L. Reno, W. Pan, J. D. Watson, M. J. Manfra, M. A. Zudov, M. Tokman, M. Erukhimova, A. Belyanin, and J. Kono, Phys. Rev. Lett. **113**, 047601 (2014).
[19] Y. Todorov and C. Sirtori, Phys. Rev. B **85**, 045304 (2012).
[20] Y. Todorov, Phys. Rev. B **89**, 075115 (2014).
[21] C. Cohen-Tannoudji, J. Dupont-Roc, and G. Grynberg, *Photons and Atoms: Introduction to Quantum Electrodynamics* (Wiley, New York, 1989).
[22] J. Keeling, J. Phys. Condens. Matter **19**, 295213 (2007).
[23] A. Vukics, T. Grießer, and P. Domokos, Phys. Rev. Lett. **112**, 073601 (2014).
[24] M. Bamba and T. Ogawa, Phys. Rev. A **90**, 063825 (2014).
[25] The last terms in Eqs. (1) and (2) are called the A^2 and P^2 terms, respectively; $(\hat{a} + \hat{a}^\dagger)$ and $\hat{\sigma}_\lambda^x$ correspond to the vector potential $\hat{A}(\boldsymbol{r})$ and the transverse atomic polarization $\hat{P}_\perp(\boldsymbol{r})$, respectively. In the presence of these terms, we do not have the superradiant phase transition in equilibrium situations even in the ultrastrong regime [24,44–48], while the laser can be realized in nonequilibrium situations regardless of whether the interaction is ultrastrong.
[26] M. Bamba and N. Imoto, arXiv:1603.00535 [quant-ph].
[27] Due to the two-level and single-mode approximations, the Hamiltonians (1) and (2) are not equivalent to each other through the transformation with the unitary operator $\hat{U} = \exp[-ig(\hat{a} + \hat{a}^\dagger)\sum_\lambda \hat{\sigma}_\lambda^x/\sqrt{N}]$, whereas the original Hamiltonians can be transformed to each other under the long-wavelength approximation [21–24]. Since $\hat{\sigma}_\lambda^x$ and $(\hat{a} + \hat{a}^\dagger)$ are commutable with $\hat{U}$, the system-environment couplings mediated by them give the same contribution in both forms. However, $\hat{\sigma}_\lambda^z$ mediating the pure dephasing is not commutable with $\hat{U}$.
[28] M. Bamba and T. Ogawa, Phys. Rev. A **89**, 023817 (2014).
[29] Since the couplings with heat baths are mediated by $\{\hat{\sigma}_\lambda^x\}$, X does not feel their influence ($\gamma_x = \gamma_{\text{pure}}$), while Y decays with the rate $\gamma_y = \gamma_\parallel + \gamma_{\text{pure}}$. We did not use the RWA to the system-environment couplings [26,28]. $X = Y = 0$ and $Z = Z_p$ are guaranteed below the threshold even in this treatment. In the same manner, the loss terms appear only in equations of motion of Π. If the RWA is applied, the results in this paper are changed quantitatively but slightly.
[30] A. Ridolfo, M. Leib, S. Savasta, and M. J. Hartmann, Phys. Rev. Lett. **109**, 193602 (2012).
[31] M. Koschorreck, R. Gehlhaar, V. G. Lyssenko, M. Swoboda, M. Hoffmann, and K. Leo, Appl. Phys. Lett. **87**, 181108 (2005).
[32] Z. Han, H.-S. Nguyen, F. Réveret, K. Abdel-Baki, J.-S. Lauret, J. Bloch, S. Bouchoule, and E. Deleporte, Appl. Phys. Express **6**, 106701 (2013).
[33] G. M. Akselrod, E. R. Young, K. W. Stone, A. Palatnik, V. Bulović, and Y. R. Tischler, Phys. Rev. B **90**, 035209 (2014).
[34] In contrast to the multimode lasers [4], the relative phases between the multiple harmonics are fixed for the laser in the ultrastrong regime, while an absolute phase can be chosen arbitrarily in the present calculation.
[35] The stability of the oscillating steady states is checked against small deviations of $|\alpha_1|, Z_0$, and $e^{-i2\theta}z_2$, where $e^{i\theta} = \alpha_1/|\alpha_1|$. The equations of motion are reduced to those of these variables, and the phase θ of α_1 is also eliminated because it is not determined by our equations of motion.

[36] Even if the interaction survives in the laser, it is different from the polariton lasers [49], i.e., the emission from polariton condensates.

[37] F. Bassani, J. J. Forney, and A. Quattropani, Phys. Rev. Lett. **39**, 1070 (1977).

[38] To make the population inversion, we use the atomic levels that interact with the two levels of interest through nonradiative transitions. These levels can be close to the two levels of interest energetically.

[39] The multistability in the conventional multimode laser shows drastic changes of the emission spectra, while peak positions are not strongly changed in the bistability originating from the lack of the RWA, as seen in Fig. 2(f).

[40] Nonclassical states of light are usually generated by applying nonlinear optical processes (showing, e.g., a bistability) to a coherent state [5,6]. For direct lasing of the nonclassical states, we basically need special tricks, such as noise-suppressed pumping [41,42].

[41] Y. Yamamoto, S. Machida, and O. Nilsson, Phys. Rev. A **34**, 4025 (1986).

[42] S. Machida, Y. Yamamoto, and Y. Itaya, Phys. Rev. Lett. **58**, 1000 (1987).

[43] O. Astafiev, K. Inomata, A. O. Niskanen, T. Yamamoto, Y. A. Pashkin, Y. Nakamura, and J. S. Tsai, Nature (London) **449**, 588 (2007).

[44] K. Rzążewski, K. Wódkiewicz, and W. Żakowicz, Phys. Rev. Lett. **35**, 432 (1975).

[45] K. Rzążewski and K. Wódkiewicz, Phys. Rev. A **13**, 1967 (1976).

[46] M. Yamanoi, Phys. Lett. A **58**, 437 (1976).

[47] V. Emeljanov and Y. Klimontovich, Phys. Lett. A **59**, 366 (1976).

[48] M. Yamanoi and M. Takatsuji, in *Coherence and Quantum Optics IV: Proceedings of the Fourth Rochester Conference on Coherence and Quantum Optics*, edited by L. Mandel and E. Wolf (Plenum, New York, 1978), pp. 839–850.

[49] A. Imamoğlu, R. J. Ram, S. Pau, and Y. Yamamoto, Phys. Rev. A **53**, 4250 (1996).